UNIVERSITY OF DELAWARE
INSTITUTE OF ENERGY CONVERSION
University of Delaware
Newark, DE 19716-3820
Ph: 302/831-6200
Fax: 302/831-6226
www.udel.edu/iec
UNITED STATES DEPARTMENT OF ENERGY
UNIVERSITY CENTER OF EXCELLENCE
FOR PHOTOVOLTAIC RESEARCH AND EDUCATION

September 23, 2005

Ken Zweibel
National Renewable Energy Laboratory
1617 Cole Boulevard
Golden, CO 80401

Re: NREL Subcontract #ADJ-1-30630-12

Dear Ken:

This report covers research conducted at the Institute of Energy Conversion (IEC) for the period July 9, 2005 to August 9, 2005, under the subject subcontract. The report highlights progress and results obtained under Task 2 ($CuInSe_2$-based Solar Cells).

TASK 2: $CuInSe_2$-BASED SOLAR CELLS

In-Line Evaporation

During the present reporting period, the focus was on the two specific issues that must be resolved for a successful commercial-scale development: (1) melt-temperature gradients, and (2) the reduction of melt-level with time. Considering how these issues arise from elemental source design, and considering their impact on process controllability, the scale-up issues can be divided into the following two components: (1) *The design issue* – where an elemental source is designed such that melt-temperature gradients are minimized, thus reducing product quality variations, and (2) *The control issue* – where the mean values of the final film quality variables are robustly controlled such that the desired set-points are achieved while simultaneously rejecting the disturbances introduced by the melt-level reduction.

To address these issues, a separate bell-jar system was assembled so that experiments can be performed without disrupting the normal operation of the pilot-scale inline system. This experimental system can accommodate one linear source boat similar to one used in the inline system. Several experiments were performed to quantify the temperature gradients in the source-boat; temperature gradients of up to 50°C were observed in the boat with asymmetric heater assembly (where both the current leads are on one end) with the lead-end being cooler than the other end. This is the boat design presently in use in the 6" web in-line system. Figure 1 illustrates the measured temperature gradient where thermocouple locations are indicated by LS,

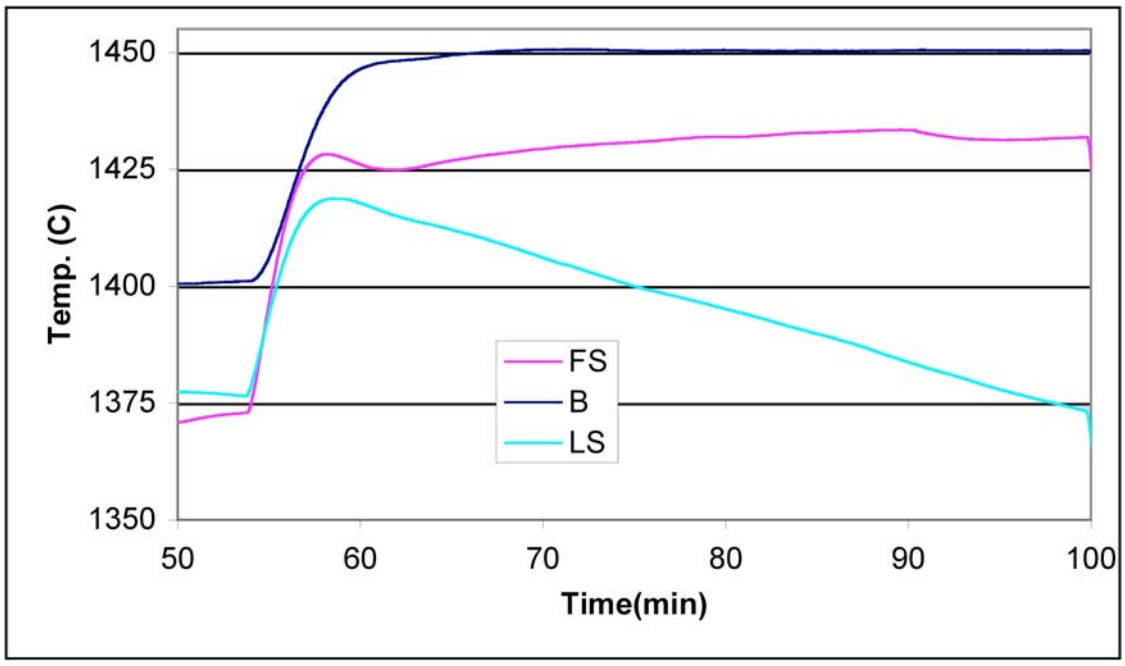

Figure 1. Temperature gradients in the linear evaporation boat; refer to text for the explanation of the legend.

FS, and B referring respectively to the power lead side, far side and the bottom. The temperature gradient was also found to be sensitive to the boat-end insulation. To determine how this kind of temperature gradient might affect the nozzle flow rates in a longer boat (for 12" wide web), preliminary Direct Simulation Monte Carlo (DSMC) simulations have been performed showing considerable flow rate difference through the two nozzles in the presence of melt-temperature non-uniformity.

A simple and effective way to get a uniform temperature distribution is to use a symmetric heater so that current leads are placed at both the ends. Provided the insulation properties are the same throughout the boat, this boat assembly should lead to equal melt-temperature beneath each nozzle and hence, equal flow rates. Experiments are in progress to observe the effectiveness of the new design. Since boat-end insulation property seems to influence the temperature uniformity within the boat, a finite-difference thermal model is being developed to study not only how insulation properties affect temperature distribution but also to combine this thermal model to the mass transfer model to study the effect of melt level reduction on the flow rates and the melt temperature.

DSMC simulations have also being performed to determine angular flux distribution through the boat nozzles – an important factor in calculating the film thickness distribution on the substrate. The simulation results have compared remarkably well with the experimental observations. This method will allow us to simulate various nozzle designs so that required angular flux distribution as well as flow rates are achieved without a need to construct a boat and experimentation.

Furthermore, effect of melt-level reduction on the nozzle flow rate can be studied using this method.

Another important issue from the process control point of view is the placement of sensors (thermocouples) so that the temperature measurements relate well to the final controlled variable (the vapor flow rates). It is found that the present scheme to place a thermocouple at the source-boat bottom is not very sensitive to the changes in the heater power (the manipulated variable). Since, the heater is placed near the source-boat lid, the changes in heater power have an immediate affect on the melt-surface temperature (and therefore the vapor flow rate), which is getting most of the energy flux from the boat lid, while the change in the source boat bottom temperature is relatively gradual.

Wide Bandgap Materials: Cu(InAl)Se_2

One of the fundamental questions regarding Cu(InAl)Se_2 films is whether they form an ordered vacancy compound (OVC) in analogy to Cu(InGa)Se_2. Cu-In-Al-Se films were deposited using the modified 3-stage process described in the May 2005 report under this subcontract and with different relative Cu/(In+Al) contents. The film compositions from EDS analyses are listed in Table I. Sample 50607 with 23 at.% Cu has the reference composition of the chalcopyrite crystal structure. The composition formulas of samples 50608 and 50610 are $Cu(In_{0.85},Al_{0.15})_{2.2}Se_{3.8}$ and $Cu(In_{0.85},Al_{0.15})_{2.9}Se_{5.0}$, respectively. An XRD profile of sample 50610 is shown in Figure 2 where characteristic peaks of the OVC type structure against the chalcopyrite structure are indicated. A similar XRD profile was obtained for sample 50608.

Table I Chemical composition of Cu(InAl)Se_2 films determined by EDS analyses.

Sample	Cu (at.%)	In (at.%)	Al (at.%)	Se (at.%)	Composition formula
50607	23	23	3	51	$Cu(In_{0.88},Al_{0.12})_{1.1}Se_{2.3}$
50608	14	27	5	54	$Cu(In_{0.85},Al_{0.15})_{2.2}Se_{3.8}$
50610	11	28	5	56	$Cu(In_{0.85},Al_{0.15})_{2.9}Se_{5.0}$

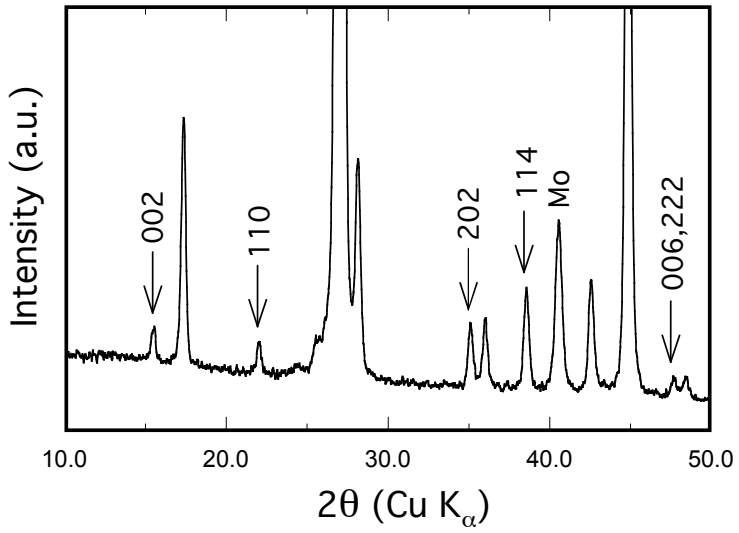

Figure 2. XRD pattern of a film with composition $Cu(In_{0.85},Al_{0.15})_{2.9}Se_{5.0}$. Peaks characteristic of the OVC structure are indicated.

Solar cell J-V parameters listed in Table II show that the cell performance decreases dramatically with the lower Cu concentrations. QE curves in the dark and under illumination are shown in Figure 3. As shown, a rough estimation of Eg can be made from the long wavelength edge of the dark QE. This indicates a widening of Eg with changing the structure type from the chalcopyrite to OVC, similar to the system of Cu-(In,Ga)-Se. Sample 50607 of the chalcopyrite type has a Eg ≈ 1.14 eV, coinciding with Eg calculated from the film composition. Sample 50608 has a wavelength tail that could be related to a mixture of the chalcopyrite and OVC phases. From the QE of sample 50610, Eg ≈ 1.32 eV can be estimated. With the 2 lower Cu content films in Figures 3(b) and 3(c), distinct difference in the QE curves in the dark and under illumination are seen corresponding to the poor device J-V performance.

Table II. $Cu(InAl)Se_2$ solar cell properties.

Sample	Eff. (%)	V_{OC} (V)	J_{SC} (mA/cm^2)	FF (%)
50607	11.5	0.577	28.8	0.692
50608	3.8	0.385	21.2	0.483
50610	0.7	0.231	9.9	0.291

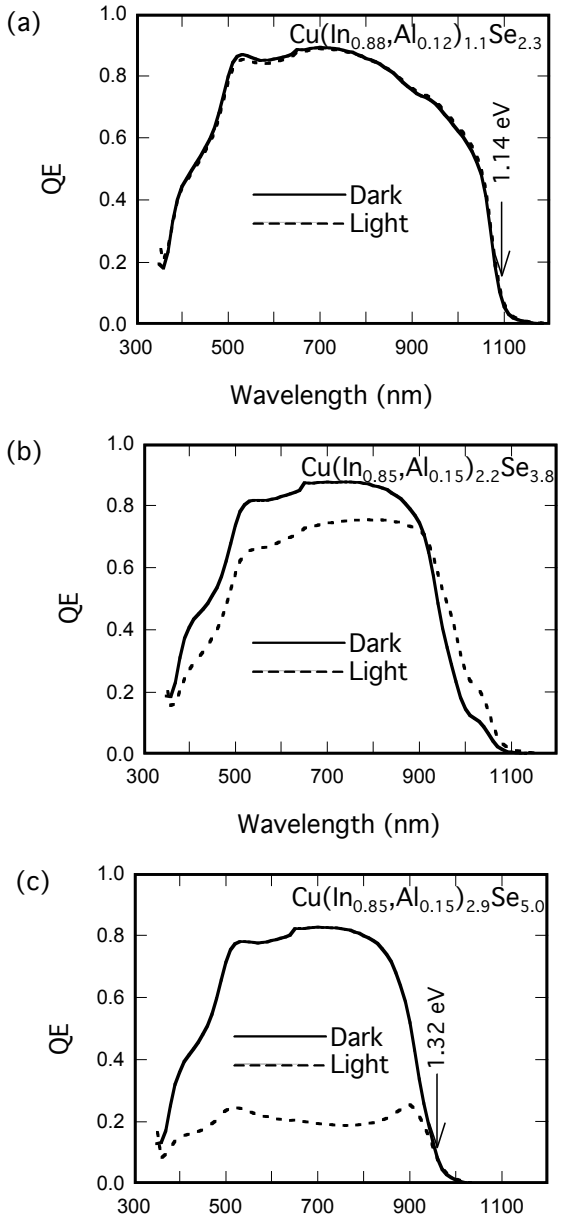

Figure 3. QE curves of Cu-In-Al-Se samples (a) 50607, (b) 50608, and (c) 50610 with compositions indicated in Table I.

$Cu(InGa)(SeS)_2$ Formation by H_2Se/H_2S Reaction

Characterization continues of the process to form $Cu(InGa)(SeS)_2$ by the two step reaction of Cu-Ga-In precursor layers in H_2Se at 400°C – 450°C followed by reaction in H_2S at higher temperature,[1,2] with the objective of understanding the composition control to increase device V_{OC}. Recent IEC results, regarding the reaction sequence, showed that after reaction in H_2Se at T = 450ºC, a Cu_9Ga_4 intermetallic phase is formed at the back of the film, which is more reactive with S than Se and quickly reacts during the H_2S stage of the growth. However, it is still unclear why Ga homogenization also occurs during the H_2S reaction. In this report a process to give uniform through-film Ga concentration is described and a $Cu(InGa)SeS)_2$ device with V_{OC} = 640 mV is demonstrated.

$Cu(InGa)(SSe)_2$ films were formed by the reaction of precursor structures with layers of 4890 Å of In on 3490 Å of $Cu_{80}Ga_{20}$ alloy sputtered on Mo/soda lime glass substrates. The precursors are reacted in atmospheric pressure Ar with 0.35% H_2Se and 0.0035% O_2 followed by reaction in Ar with 0.35% H_2S and 0.0035% O_2. Key process variables to control the film composition are the temperature and duration of the two reaction steps. Four time-temperature profiles were investigated and are summarized in Table III. Processes 1 and 2 using a 400ºC H_2Se reaction were both found to be incompletely reacted after the 500ºC H_2S reaction, and intermetallic phases were detected by XRD. Process 3, utilizing a 30 min H_2Se reaction at 450ºC, gave Ga/(In+Ga) = 0.08 by EDS, less than the value of 0.2 in the precursor. It is suspected that the H_2Se reaction was carried too far, so that there was insufficient Cu_9Ga_4 for Ga homogenization. Process 4, with a 15 min H_2Se reaction at 450ºC followed by a 30 min 550ºC H_2S reaction, produced the high performance $Cu(InGa)(SeS)_2$ film characterized below.

Table III. Summary of investigated time-temperature profiles for two-step reaction of metallic precursors.

Process	H_2Se reaction	H_2S reaction	Ga/(Ga+In)	S/(S+Se)	Comments
1	400ºC 30 min	500ºC 15 min	0.21	0.47	Residual intermetallics Shorted devices
2	400ºC 45 min	500ºC 15 min	0.16	0.46	Residual intermetallics, Shorted devices
3	450ºC 30 min	550ºC 15 min	0.08	0.25	Ga not homogenized, Flaking in CdS bath
4	450ºC 15 min	550ºC 30 min	0.17	0.28	Ga homogeneous Device V_{OC} =0.64 V

The composition of the reacted film from process 4 measure by EDS gave Cu/(In+Ga) = 0.90, Ga/(In+Ga) = 0.17, and S/(Se+S) = 0.28. The relative Cu, Ga, and In compositions match the precursor. The XRD spectrum, shown in Figure 4, indicates a high degree of compositional uniformity within the $Cu(InGa)(SeS)_2$ phase, as evidenced by the narrow peak width. All peaks

are indexed by the Mo and Cu(InGa)$(SeS)_2$ except a small peak at 21.8º which might indicate residual In(SSe) within the film. Compositional depth profiles measured by Auger electron spectroscopy (measured by Craig Perkins at NREL) are shown in Figure 5. These indicate a uniform through-film Ga/(In+Ga) profile but a steep S gradient near the surface.

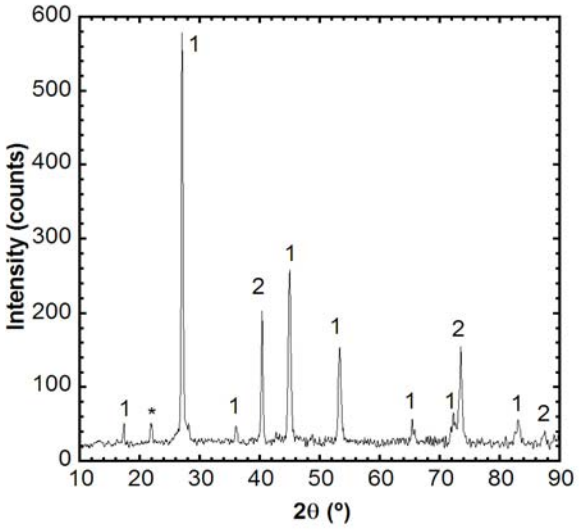

Figure 4. XRD spectrum of Cu(InGa)$(SeS)_2$ from process 4. (1 = Cu(InGa)$(SeS)_2$; 2 = Mo; * = unknown).

Devices were fabricated using a SL/Mo/Cu(InGa)$(SeS)_2$/CdS/ZnO/ITO/Ni-Al grid structure. The best device had efficiency = 13.2 % with V_{OC} = 0.641 V, J_{SC} = 31.6 mA/cm^2, and FF = 65.1 %. The relatively poor FF may be due to a barrier-to-collection of electrons caused by the steep S gradient.

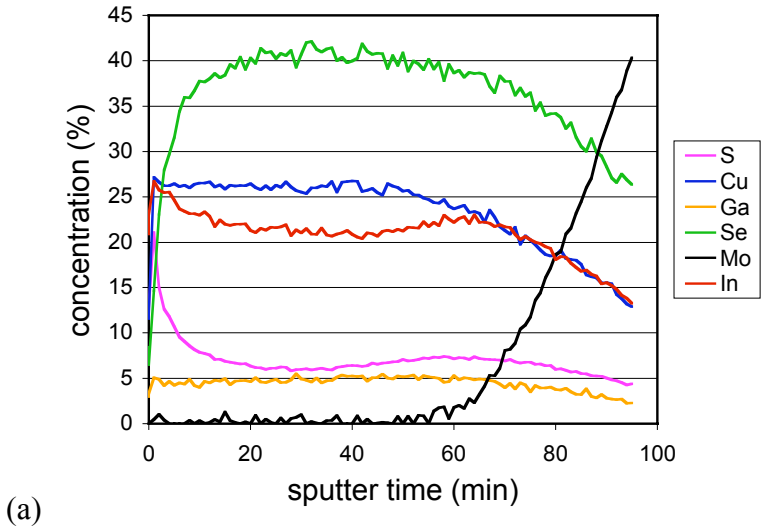

(a)

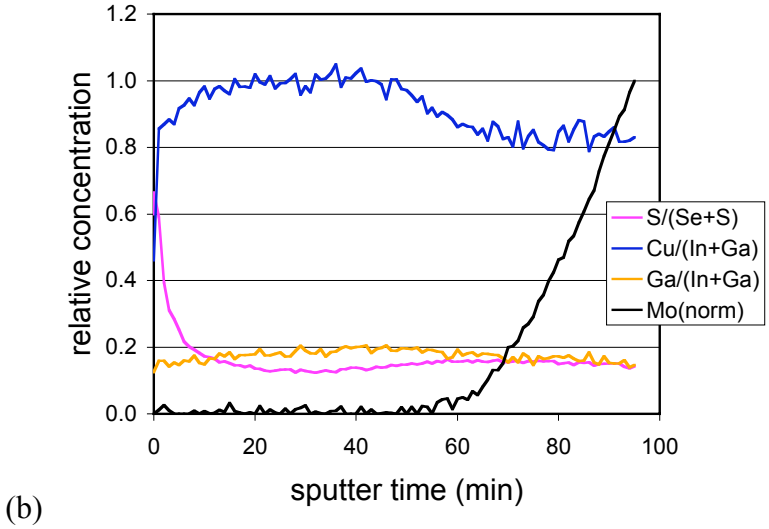

(b)

Figure 5. Compositional depth profile of Cu(InGa)$(SeS)_2$ formed by two-step reaction in H_2Se and H_2S process 4.

Fundamental Materials and Interface Characterization

An aqueous Br-etch[3] has been used to level and thin Cu(InGa)Se_2 films, and we previously showed in the November 2004 report under this subcontract that the this provides a smooth surface suitable for detailed optical analysis using spectroscopic ellipsometry (SE). It was also shown that a Se-rich surface layer left by the Br-etch[4] can be removed with either a KCN etch or by thermal annealing enabling devices to be fabricated. Further experiments have been done to explore the use of these etches to vary thickness in a well controlled manner, enabling more fundamental study of the effects of reducing Cu(InGa)Se_2 thickness (d) and characterization of optical reflection at the Mo/Cu(InGa)Se_2 contact.

One issue for characterizing the etched films is the precise determination of the Cu(InGa)Se_2 thickness. Several possible methods have been evaluated including measuring the change in mass of the film, cross-sectional SEM images, and extinction of the Mo peak in the EDS spectrum. A simple, non-destructive method is to measure the optical reflection (R) and determine thickness from the optical interference fringes in the transparent region at energies below the bandgap using a procedure reported by Swanepoel.[5] This requires knowing the refractive index as a function of wavelength which we have determined using SE.[6] Figure 7 shows the total reflection for an as-deposited Cu(InGa)Se_2 film with Ga/(In+Ga) = 0.3 and films after 2 and 4 min

Br etches in an aqueous 0.03M Br solution at room temperature. The as-deposited film has lower R in the absorbing region $\lambda < 1000$ nm and smaller amplitude of the interference fringes in the transparent region at higher λ. This is attributed to the scattering due to the rough surface of the as-deposited film. The spacing of the maxima or minima in the spectra increases with increasing etch time as the films become thinner and were used to determine the thicknesses listed. The change in thickness determined with this method is shown in Figure 8 for etch times up to 4 min and the slope gives an etch rate of 0.2 μm min^{1}.

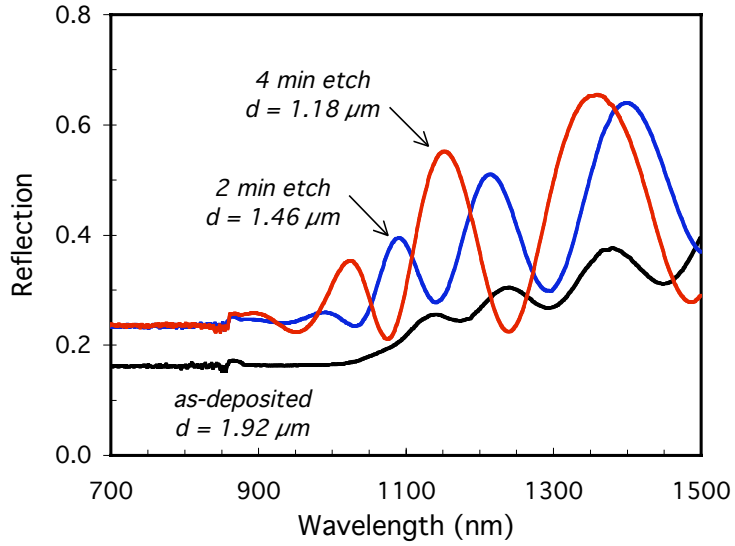

Figure 7. Optical reflection of as-deposited and Br-etched Cu(InGa)Se_2 films and the thicknesses obtained from the interference fringes.

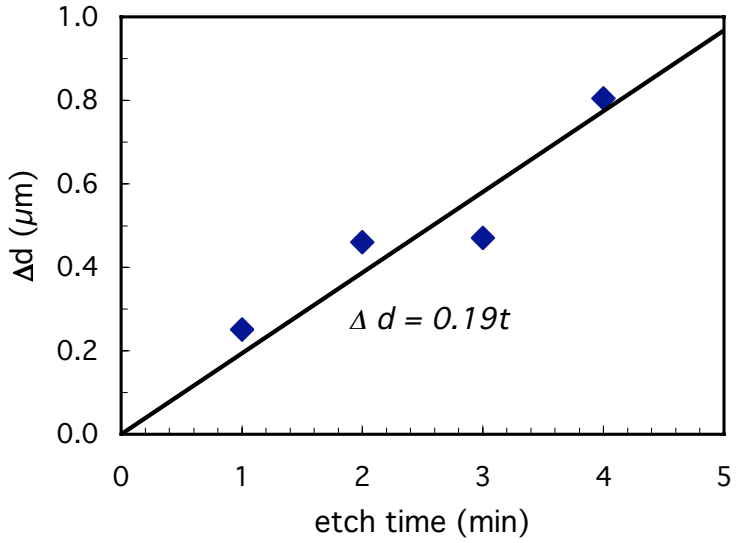

Figure 8. Change in thickness for different Br-etch times.

Samples from a single Cu(InGa)Se_2 run were etched for 1, 2, 3, and 4 min and, after R was measured, devices were fabricated. The resulting thickness and device parameters are listed in Table III. All the etched films had slightly lower J_{SC} than the un-etched sample, which can be attributed to higher reflection losses with the specular etched films. V_{OC} was also slightly lower but the reason is not known.

Table III. Cu(InGa)Se_2 thickness and device J-V parameters as a function of Br-etch time of the Cu(InGa)Se_2 absorber layer.

Sample #	etch time (min)	Cu(InGa)Se_2 d (μm)	η (%)	V_{OC} (V)	J_{SC} (mA/cm^2)	FF (%)
33930.22	as-dep	1.92	14.5	0.621	31.1	75.0
33930.12	1	1.67	11.8	0.582	28.1	72.1
33930.13	2	1.46	12.7	0.593	28.6	74.7
33930.21	3	1.33	13.8	0.602	30.5	75.4
33930.23	4	1.18	12.1	0.583	28.7	72.5

Best regards,

Robert W. Birkmire
Director

RWB/bj
cc: Gerri Hobbs, UD Research Office
Carolyn Lopez, NREL
Paula Newton
Erten Eser
William N. Shafarman

1. K. Kushiya, et al. *Sol. Energy Mat. Sol. Cells* **49**, 277 (1997).
2. V. Alberts, J. Titus, R.W. Birkmire, *Thin Sol. Films* **451-2**, 207 (2004).
3. R.W. Birkmire, B.E. McCandless, *Appl. Phys. Lett.* **53**, 140 (1988)
4. B. Canava, J.F. Guillemoles, J. Vigneron, D. Lincot, A. Etcheberry, *J. Phys. Chem. Sol.* **64**, 1791, (2003).
5. R. Swanepoel, *J. Phys. E* **16** 1214 (1983).
6. P.D. Paulson, R.W. Birkmire, W.N. Shafarman, *J. Appl. Phys.* **94**, 879 (2003).